Chinese Journal of
POLYMER SCIENCE

RESEARCH ARTICLE

https://doi.org/10.1007/s10118-025-3345-3
Chinese J. Polym. Sci. **2025**, *43*, 1576–1583

Relaxation-reversed Phase Transition of Poly(butylene succinate)

Jia-Liang Qiao, Xin-Yu Liu, Ying-Zhuo Liu, Gui-Qiu Ma*, and Zhe Ma*

School of Materials Science and Engineering, State Key Laboratory of High Performance Roll Materials and Composite Forming, Tianjin Key Laboratory of Composite and Functional Materials, Key Laboratory of Organic Integrated Circuits, Ministry of Education, Tianjin University, Tianjin 300072, China

Electronic Supplementary Information

Abstract The stretching-induced phase transition of biodegradable poly(butylene succinate) (PBS) was explored using a combination of mechanical testing and *in situ* wide angle X-ray diffraction characterization. The phase transition from α phase to β phase can be effectively triggered by severe stretching, in which the threshold strain is dependent on the PBS crystallites. Interestingly, this α-β phase transition can be reversed immediately once mechanical stretching begins to be released. It should be pointed out that the finish of β-α phase transition reversed, corresponding to the disappearance of the generated β phase, does not necessarily need the external stretching to completely release. For the relaxation-reversed phase transition, the evolution of the normalized β-phase fraction exhibited a similar correlation with the stress released. It was indicated that the decay kinetics followed a stretching-dominant mechanism, and the amount of β phase generated just prior to relaxation had a negligible influence on the reversed phase transition.

Keywords Wide angle X-ray diffraction (WAXD); Phase transition; Stretching; Relaxation

Citation: Qiao, J. L.; Liu, X. Y.; Liu, Y. Z.; Ma, G. Q.; Ma, Z. Relaxation-reversed phase transition of poly(butylene succinate). *Chinese J. Polym. Sci.* **2025**, *43*, 1576–1583.

INTRODUCTION

For semicrystalline polymers, the mechanical deformation that is often applied during the processing and/or use of a product may lead to significant structural evolution and consequently vary the material performance.[1] Among the various structural evolutions, the stretching-induced phase transition is a quite general and important phenomenon observed in many polymers.[2–8] For example, in polybutene-1 (PB), stretching can trigger a phase transition from the tetragonal phase into the trigonal phase, resulting in an increase in the strain hardening modulus by nearly two orders of magnitude.[9–11] For poly(vinylidene fluoride) (PVDF), stretching can induce a pseudo-orthorhombic phase with excellent thermal stability to transform into an orthorhombic phase with high piezoelectricity.[12–19] However, in some other polymers, such a stretching-induced new phase may recover as the external deformation is diminished.[20–23] In poly(butylene terephthalate) (PBT), a conformational transition from α phase to β phase is observed by applying tensile stress, whereas those crystallites of β phase gradually revert to the initial α phase in the relaxation process.[24–25] During the past decades, many excellent investigations have been devoted to stretching-induced phase transition, but the corresponding reversed phase transition with relaxation has attracted much less attention and is still far from a comprehensive understanding.

The stretching-reversed phase transition may experience direct and indirect processes. Yokouchi *et al.* studied the reversible transition of two crystalline forms in PBT and found that the stretching-generated β phase was unstable and could revert to the original α phase once the stress was removed.[25] This reversible phase transition during stretching can primarily be attributed to the stretching-induced conformational adjustment of the molecular chains and relaxation-induced subsequent recovery upon stress removal.[26–30] It should also be noted that in some polymers, the elevation of temperature was required to trigger the occurrence of the reversed phase. For poly(butylene adipate-co-terephthalate) (PBAT), the stretching-generated β phase can directly transform back to α phase only when the stress was removed, and at the same time, the un-stretched sample was annealed at 100 °C.[31] In addition to the above solid-solid phase transition, Men *et al.* also found that in PB, stretching easily generated a trigonal phase from the tetragonal phase at room temperature, and further stretching at an elevated temperature of 115 °C can re-obtain the tetragonal phase through the melt-recrystallization pathway.[32,33] Clearly, the correlation between the phase transition and external deformation largely varies with the crystalline features.

Semicrystalline poly(butylene succinate) (PBS) is a representative biodegradable polyester with excellent toughness and safety for food contact and is an attractive candidate for environmentally friendly packaging solutions.[34–42] Mean-

* Corresponding authors, E-mail: magq@tju.edu.cn (G.Q.M.)
E-mail: zhe.ma@tju.edu.cn (Z.M.)

Received February 24, 2025; Accepted March 24, 2025; Published online May 8, 2025

while, PBS is a polymorphic polymer, and its different phases could transform between each other. Under quiescent conditions, PBS adopts a monoclinic *α* phase crystalline structure, which can transform into a monoclinic *β* phase by severe stretching.[43] In a pioneering work, Ichikawa *et al.* studied the stretching-induced morphology of PBS fibers and found that the *α*-*β* phase transition was triggered by the application of tensile stress and reversed with subsequent unloading.[44] Their detailed structural analysis on PBS also showed that the *α* phase unit cell has the following parameters: a = 0.523 nm, b = 0.912 nm, c = 1.090 nm, and β = 123.98°, while the *β* phase unit cell is in the dimension with a = 0.584 nm, b = 0.832 nm, c = 1.186 nm, and β = 131.68°.[20,43–46] To properly pack into the crystal lattice, *α* phase has a conformation of $T_7GT\bar{G}$ and *β* phase has a conformation of T_{10}, where *T*, *G*, and $\bar{G}$ denote trans, gauche, and minus gauche, respectively.[44,46] It is known that the occurrence of stretching-induced phase transition may require various stretching strengths. Zhou *et al.* found that in PBAT, the *α*-*β* transition starts quickly with increasing strain of stretching.[31] Differently, the *in situ* wide angle X-ray diffraction characterization performed by Liu *et al.* disclosed that the *α*-*β* phase transition of PBS began in the strain hardening stage, where oriented microfibrillar structures were formed, although these two phases are both of monoclinic modification.[23] On the other hand, it was recognized that for PBS, the removal of stress alone can induce the reversed transformation of the stretching-generated *β* phase back to the original *α* phase, which is different from the case of the above PBAT, which required both stress removal and temperature elevation. However, the detailed process of this relaxation-induced *β*-*α* phase transition is unclear.

In this work, the stretching-triggered phase transition of PBS and especially its corresponding relaxation-induced reversed process were studied with the *in situ* wide angle X-ray diffraction. The *α*-*β* phase transition started after severe stretching was applied, whereas the reversed *β*-*α* process began immediately with the decrease of stress. What is more interesting is that the complete decay of *β*-phase crystallites back to the initial *α*-phase crystallites can be achieved by partial unloading of stretching. For various fractions of *β* phase in the total crystallites to be recovered, their decay kinetics seem to follow a similar correlation with the strength of the relaxing stretching.

EXPERIMENTAL

Materials

The PBS studied in this work was obtained from Xinjiang Blueridge Tunhe Polyester Co., Ltd. The molecular weight was measured by Gel Permeation Chromatography (GPC) with an Agilent PL-GPC 50 instrument using HFIP (1,1,1,3,3,3-hexafluoro-2-propanol) as the eluent, which was combined with a Refractive Index detector. The polystyrene was used as the standard at 25 °C with a flow rate of 1.0 mL/min. The weight-averaged molecular mass was 116 kDa and the polydispersity index was approximately 2.5.

The PBS granules were first hot-pressed into sheets and held at 180 °C for 10 min to clean the thermal history. Next, the tensile samples were prepared by two different thermal protocols. To prepare the isothermally crystallized samples, the sheets were quickly placed in a water bath set at 25, 50, 70 and 90 °C for crystallization (referred to as PBS-IT25, PBS-IT50, PBS-IT70, and PBS-IT90, respectively). In addition, to prepare the quenched and annealed samples, the molten sheets were quickly quenched in an ice/water mixture, which was subsequently annealed at 25, 50, 70 and 90 °C for 4 h (referred to as PBS-ANN25, PBS-ANN50, PBS-ANN70, and PBS-ANN90, respectively). The samples were cut into dumbbell-shaped strips of 0.5 mm thickness for mechanical experiments.

Mechanical Measurement

The mechanical property tensile tests were performed using the Linkam TST350 tensile tester. The tensile speed was 5 μm·s^{-1}. The specific stress-strain curves are shown in Fig. S1 (in the electronic supplementary information, ESI).

Wide Angle X-ray Diffraction (WAXD) Characterization

In situ wide-angle X-ray diffraction (WAXD) measurements were performed on a SAXSFocus 3.0 system (GKINST, China). The setup consisted of a multilayer focused Cu K*α* X-ray source (MFOCUS, GKINST, China). The X-ray wavelength was 0.154 nm. The two-dimensional (2D) images were recorded using an EIGER2 R 1M detector, which has a resolution of 1062 × 1028 pixels (pixel size of 75 μm × 75 μm). The sample-to-detector distance of WAXD was 63 mm. The exposure duration for each WAXD pattern was 300 s.

Prior to stretching, the crystallite structures were examined for the un-deformed samples. The WAXD results are shown in Fig. 1. The diffraction signals of the same characteristic (020)/($\bar{1}$11), (110) and (111) crystallographic planes were observed, which demonstrated the formation of the sole *α* phase in all PBS samples.[22,44]

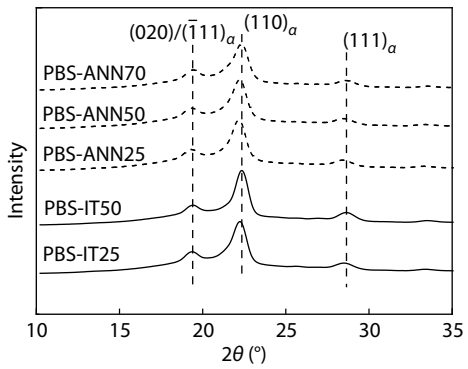

Fig. 1 The 1D WAXD patterns of the isothermally crystallized samples (solid lines) and the annealed samples (dash lines).

Considering the fact that stretching induces the appearance of highly oriented crystallites (Fig. 2a), only the diffraction signals of the ($\bar{1}$03)$_\alpha$ and ($\bar{1}$03)$_\beta$ crystallographic planes over the meridian region (azimuth range from −15° to 15°) in the 2D patterns were integrated. The multi-peak fitting method was employed to obtain the fractions of various phases (Fig. 2b). The fraction of *β* phase was estimated by

$$f_\beta = \frac{A_\beta}{A_\beta + CA_\alpha} \quad (1)$$

where A_α and A_β are the integral areas of the diffraction peaks

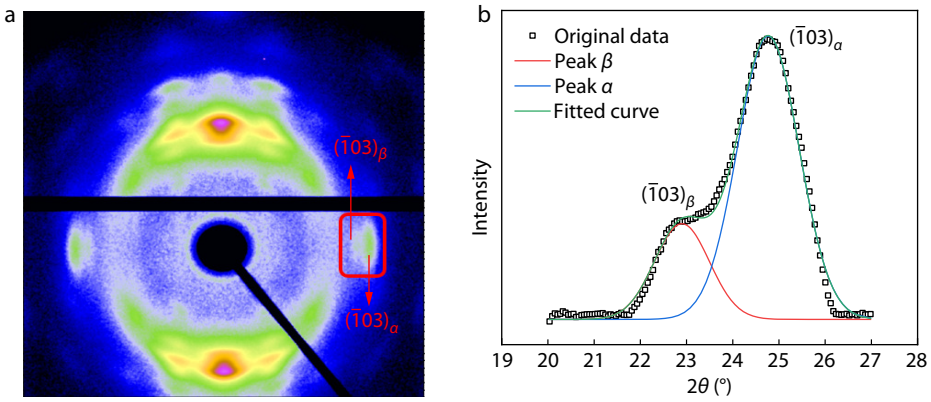

Fig. 2 (a) The 2D WAXD pattern of stretched PBS, where the stretching direction was horizontal. (b) The corresponding 1D integrated curve and the applied peak fitting method to quantify various phases.

of the *α* phase ($\bar{1}03$) and the *β* phase ($\bar{1}03$), respectively. A factor *C*=0.37 was employed to correct the diffraction intensity difference between crystallographic planes.[23, 44]

RESULTS AND DISCUSSION

To track the stretching-induced evolution, the *in situ* wide-angle X-ray diffraction was employed. Taking PBS-IT25 as an example, Fig. 3(a) shows the stretching-induced structural evolution together with the mechanical response. Prior to stretching, the original crystallites in *α* phase were isotropic (Fig. 3a). With the application of stretching, the crystallites started to rotate and became slightly oriented, as indicated by the in-homogeneous distribution of diffraction peaks over the azimuthal angle. As the stretching reached an increased strain of around 100%, the diffraction signals of *α*-phase $(110)_\alpha$ and $(020)_\alpha$ crystallographic planes became concentrated in the equatorial region. The orientation of the initial crystallites in *α* phase gradually developed further with continuous stretching, while the distinct signal of the $(\bar{1}03)_\beta$ crystallographic plane belonging to *β* phase could appear in the meridional region, demonstrating that *α* phase began to transform into *β* phase. Fig. 3(b) presents the detailed 1D WAXD curves that were mainly integrated over the meridional region. For the original *α* phase, the $(110)_\alpha$ and $(020)_\alpha$ intensities decreased by stretching, which was mainly caused by the continuous orientation evolution towards the equatorial region. Differently, the $(\bar{1}03)_\alpha$ intensity of *α* phase changed in a distinct manner, which was mainly associated with a distinct orientation into the meridional region. Then, the *α* phase $(110)_\alpha$ intensity became absent completely in the equatorial region at 200%. Afterwards, the $(\bar{1}03)_\beta$ intensity of *β* phase was detected at a stretching strain of 240%. Once triggered, the *α*-*β* phase transition proceeded with the continuous stretching. The WAXD intensity of the $(\bar{1}03)_\beta$ crystallographic plane that originated from the newly generated *β* phase, continued to increase until fracture.

Normally, stretching-induced phase transition corresponds to the re-arrangement of packed stems by adjusting the positional ordering and/or helical conformation.[26,47] Actually, the crystal lattice as a whole can also be stretched to rotate to align along the stretching direction. It was recently disclosed in polybutene (PB) that these two structural evolutions at various length-scales may happen simultaneously, where the phase transition from tetragonal into trigonal modification could happen mainly within the off-axis oriented crystallites.[48] After the finish of this phase transition, the transformed trigonal crystallites of PB rotated further and became highly oriented along the stretching direction. In this work, the orientation of PBS *α* phase proceeds earlier than its phase transition into *β* phase, which always requires the initial *α* phase to be completely oriented and aligned along the stretching direction.

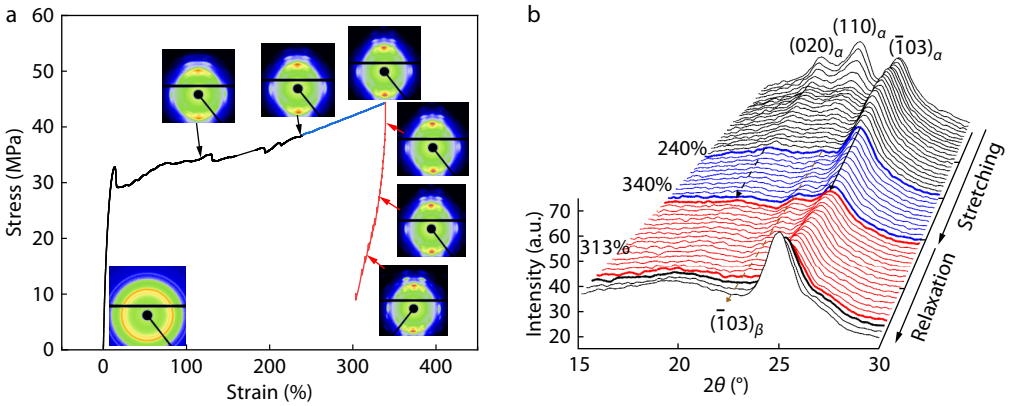

Fig. 3 (a) Selected *in situ* 2D WAXD patterns and (b) the corresponding 1D patterns obtained during stretching of PBS-IT25. The stretching direction is horizontal.

https://doi.org/10.1007/s10118-025-3345-3

Furthermore, it has been reported that the stretching-generated β phase might decay back into the original α phase after the mechanical stress was unloaded.[1, 27] However, the detailed evolution of this reversed phase transition remains mysterious. Consequently, the relaxation-induced reversible phase transition was explored by the *in situ* WAXD in this work. Our experiment showed that PBS-IT25 has a large fracture strain of around 350% (black lines in Fig. S1 in ESI), and the relaxation process did not start until a quite large strain of 340% to obtain β phase as much as possible (Fig. 3a). It was noteworthy to see that within the unloading process, the $(\bar{1}03)_\beta$ intensity of the newly transformed β phase decreased, but the $(\bar{1}03)_\alpha$ intensity of α phase increased (red curves of Fig. 3b). Eventually, β phase $(\bar{1}03)_\beta$ intensity could completely disappear during unloading. This means that the crystallites in β phase completely transformed back into α phase. The quantitative evolution of β phase during stretching and recovery was summarized in Fig. 4(a). Importantly, the complete recovery from β into α phase just needs a partial relaxation condition with a strain = 313% and a stress = 15.6 MPa. In summary, three quantitative aspects were disclosed for the inversed phase transition. First, those generated β phase immediately started to transform back to initial α phase once the stretching was unloaded. Secondly, it is intriguing to quantitatively identify a partial relaxation condition to allow all of the generated β phase to completely transform back. Thirdly, the quantitative evolution of the inversed β-α phase transition seems to exhibit a strong correlation with the relaxed stretching.

However, a question may arise whether this specific incomplete relaxation condition of decaying all β phase is determined by the kinetics of the aforementioned β-α transition during unloading. Then, another constant-stress protocol was applied to examine the contribution from kinetics of the reversed β-α phase transition. In this type of experiment, PBS-IT25 crystallites were stretched to two representative stresses of 38.7 and 42.4 MPa, corresponding to the low and high fractions of β phase, respectively. The WAXD characterization was performed to disclose the evolution of those generated β phase changes under the fixed stress. It is striking to find that the β-phase content did not change under constant stress, even the constant-stress duration lasted as long as 14 h (Fig. 4b). It was implied that the phase transition kinetics under constant stress is negligible.

In addition, the isothermal temperatures of preparing crystallites were elevated to 50, 70 and 90 °C, in order to tune the crystallites to be transformed. However, only PBS-IT50 was stretchable, while PBS-IT70 and PBS-IT90 were so brittle that were not suitable for *in situ* WAXD experiments (Fig. S1 in ESI). Thus, Fig. 5 presents the stretching-induced reversible α-β transition of PBS-IT50. It is seen that the $(110)_\alpha$ intensity of original α phase decreased gradually with stretching, but before the complete disappearance of α phase, the $(\bar{1}03)_\beta$ diffraction signal of β phase quickly appeared at strain = 210%. This is different from the above PBS-IT25 that the $(\bar{1}03)_\beta$ diffraction signal of β phase appears after the disappearance of α phase. In this case, the starting strain of α-β transition cannot be identified, due to the fact that their two crystallographic planes are too close to be distinguished. Only after strain = 210%, the intensity of the $(020)_\alpha$ crystallographic plane completely disappears in the meridional region. This means that the precise fractions of β phase can only be determined for the relatively late stretching stage with a strain equal to and larger than 210%. However, these results are sufficient to demonstrate that PBS-IT25 and PBS-IT50 have distinct strain thresholds for triggering α-β phase transition, of which the former is 240%, but the latter is much smaller than 210%. During stretching, β phase was more easily generated in PBS-IT50 than in PBS-IT25. This was confirmed by the fact that at the identical strain of 340%, the fraction of β phase reaches 0.63 in PBS-IT50, while that was 0.55 in PBS-IT25. More interestingly, the fraction of β phase in the recovery (red curves) gradually decreased and completely disappeared at the strain of 310% (Fig. 5a).

From the above results of PBS-IT25 and PBS-IT50, it was found that the stretching-induced appearance of β phase can be reversed by a partial relaxation. To examine the availability of the relaxation-induced β-α phase transition, an alternative preparation approach, that includes the two sequential quenching and annealing steps, was also utilized, preparing more stretchable PBS crystallites. Fig. 6(a) shows the stretching-induced reversible phase transition of PBS-ANN25 and PBS-ANN70 as the representative. Considering the crystal lattice as a whole, the crystallites change from isotropic texture

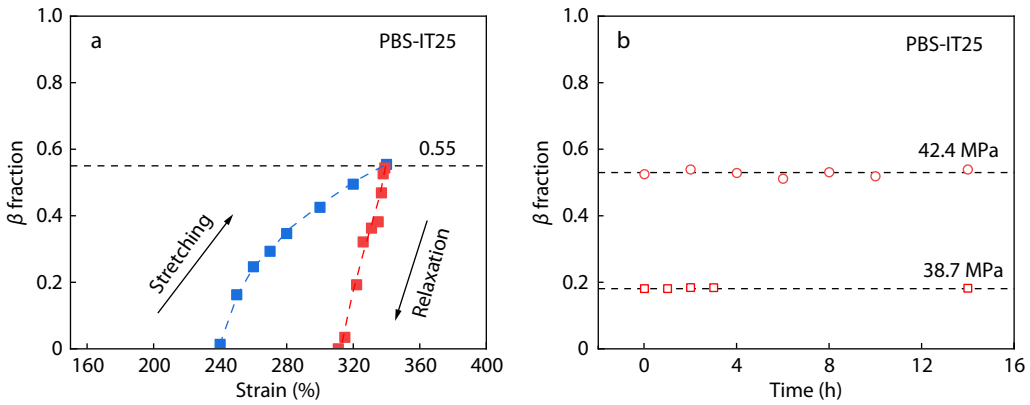

Fig. 4 (a) The evolution of PBS-IT25 β phase fraction during stretching and relaxation. The blue points represent the stretching process, while the red indicate the relaxation process. (b) The unchanged fractions of PBS-IT25 β phase under constant stresses for long durations.

https://doi.org/10.1007/s10118-025-3345-3

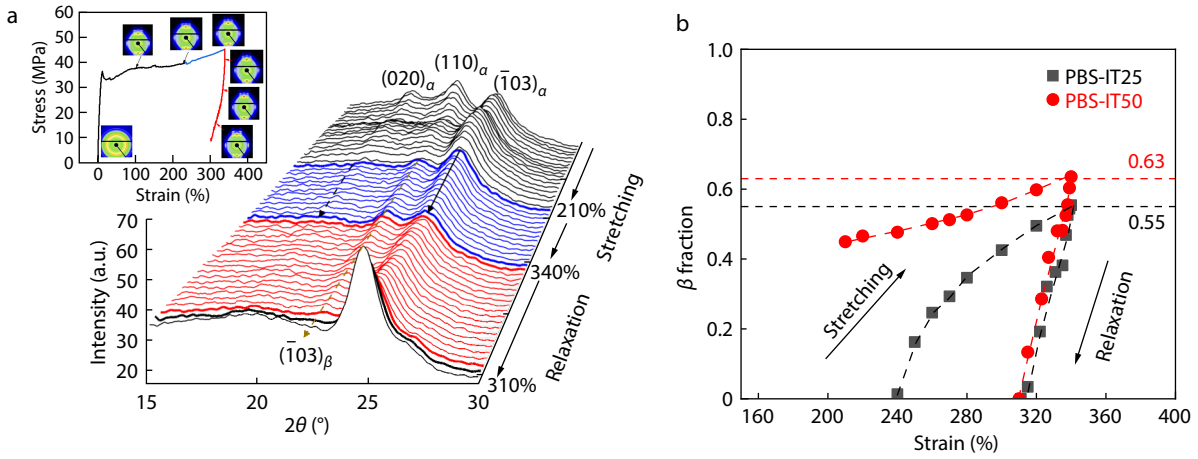

Fig. 5 (a) Selected *in situ* WAXD results and (b) the β fraction of PBS-IT50 (red symbols) during stretching and relaxation, where the results of PBS-IT25 (black symbols) were given as a reference.

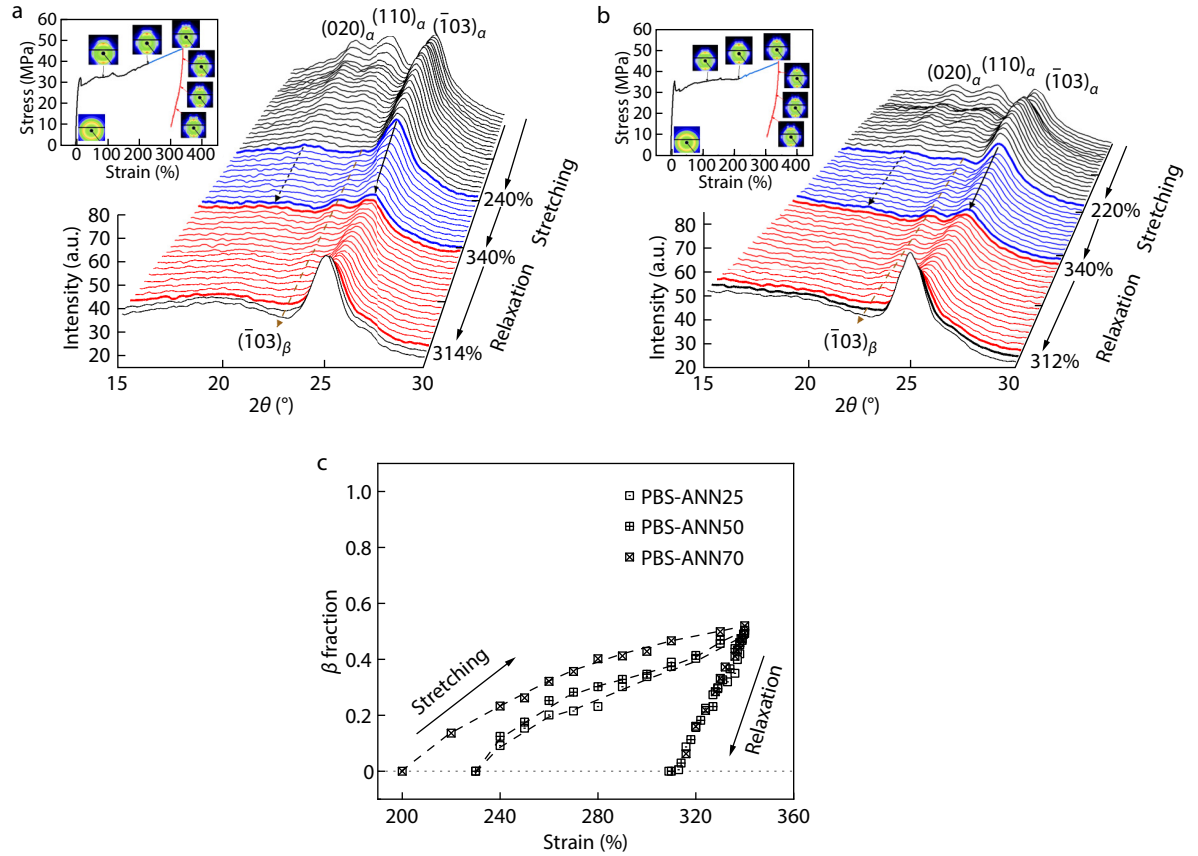

Fig. 6 Selected *in situ* 2D WAXD patterns plotted with stress-strain curves and the corresponding 1D WAXD patterns of (a) PBS-ANN25 and (b) PBS-ANN70. (c) The determined fraction of β phase in PBS-ANN25, PBS-ANN50, and PBS-ANN70 during stretching and relaxation. The stretching direction is horizontal.

into a highly oriented structure by stretching. Concerning the crystal lattice in a smaller length-scale, it was found that the weak signal of the $(\bar{1}03)_\beta$ crystallographic plane appeared in the meridional region (blue lines). For the original α phase in these PBS-ANN samples, the crystallite orientation developed outwards from the equatorial region much faster than its phase transition into β phase, so the precise critical strain of the starting α-β phase transition can be determined. As shown by Fig. 6(c), PBS-ANN25 and PBS-ANN50 have a similar critical transition strain of 240%, which is larger than 220% of PBS-ANN70. As stretching was continuously implemented, the β-phase fraction of PBS-ANN70 was higher than that of PBS-ANN25 and PBS-ANN50, which afterwards reaches comparable levels at a large strain of 340%. Interestingly, the relaxation-induced evolution of β phase follows a similar dependence on the relaxation for various annealed samples.

https://doi.org/10.1007/s10118-025-3345-3

It is known that due to stretching, the stems packed within the crystal could be elongated along chain axis, and the transformed β phase possesses a relatively larger value of the unit cell parameter c than the original α phase (1.186 nm versus 1.090 nm).[44,45] This means that a minimum strain of around 8.8% is needed to meet the geometry requirement of α-β phase transition. As expected, all critical strains of forming β phase are well above this basic strain solely for crystal lattice, of which a majority was consumed by the crystallite fragmentation and the relative movements. On the other hand, the reversed α-β transition seems to finish at the incomplete stretching conditions with a strain of around 310% and a stress of around 15.6 MPa. It was implied that in addition to the decay of β phase, other relaxation event such as amorphous network happens also. The kinetics of reversed transform of β phase back to α phase was examined by normalizing the relaxation-induced decay of β phase fraction, which shows that the β-phase fraction before relaxation had a negligible influence on the reversed phase transition (Fig. 7b). Consequently, it is interesting to see all the quantitative processes of the reversed β-α phase transition follow a similar mechanism. The β phase immediately started to transform back to α phase once the relaxation began. On the other hand, the disappearance of β phase does not necessarily need the elastic strain and elastic stress to completely release. This is consistent with the stretching-induced appearance of β phase, where severe stretching is required to trigger the phase transition from α phase. The serial model was developed to understand the stretching-induced formation of β phase from α phase in PBS. In addition to the crystalline part, two types of amorphous components could exist in the stretched system, of which one is a series component connected to crystallites and the other one is a parallel component surrounding crystallites. The results of this work further indicate that for the β-α process of interest, the crystalline part seems to include crystallites in both α and β phases, which are connected also series. With crystallites, the series amorphous component could be the intrinsic alternatively connected amorphous layers, while the parallel amorphous component might be the network built by the entangled chains as a whole. Starting from the initial isotropic texture, the complex stretching-induced structural evolution has to experience several steps, including destruction of the whole crystallite aggregates, fragmentation and slippage of lamellar crystallites, formation of microfibrillar structures, and effective stretching of the entangled amorphous network.[33,49] Thus, the substantial formation of β phase by stretching implies that the whole system was highly stretched. Differently, the relaxation process is much simpler, where some of the above events are permanent and cannot be recovered. For example, the generated fibrillar crystallites remained in the stress-relaxed system, which is consistent with persistent highly oriented crystallites. For PBS, the reversed phase transition exhibits to an extent like a special formation of elastic deformation. Once stretching was interrupted to unload, these generated β phase not only stopped forming but also decayed, where the decay process showed a direct correlation with the recovered stretching. In addition, the partial relaxation is able to allow β phase completely to change back, thus the corresponding residual stretching should be undertaken by the amorphous components and the crystallites in recovered α phase. The residual stretching after relaxation-decayed β phase is consistent with the requirement of critical condition sufficient to generate β phase during stretching, where the original components should be stretched to transfer sufficiently external stimuli to trigger phase transition.

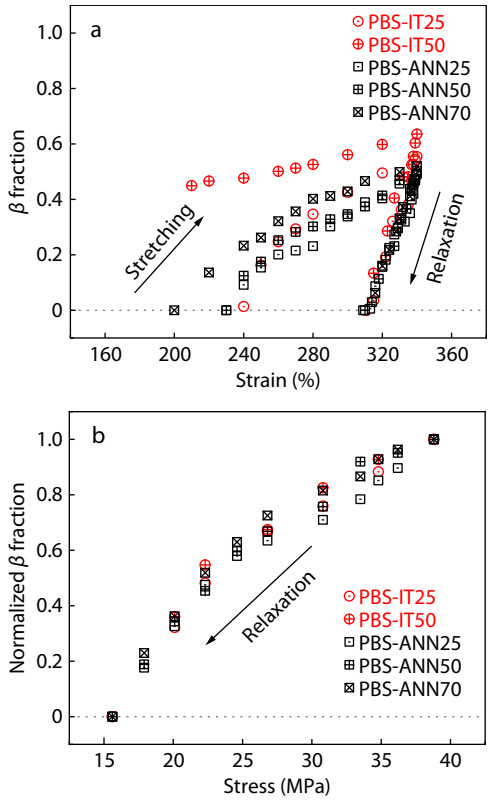

Fig. 7 (a) Plot of stretching-induced β phase as a function of strain. (b) Plot of normalized β-phase fraction as a function of stress for the relaxation process.

CONCLUSIONS

In this work, the detailed evolution of the reversible PBS phase transition between α and β phases was investigated by employing the time-resolved wide angle X-ray diffraction method. For the stretching-triggered PBS transition from α phase into β phase, a threshold of severe stretching was required, which is different from the case of PBAT, in which the phase transition started immediately with stretching. For example, the PBS α-phase crystallites prepared by isothermal crystallization at 25 °C require a large strain of around 240% to trigger the phase transition into β phase. However, for all crystallites prepared in this work, α phase of PBS can only be partially transformed into β phase, even until sample fracture. Next, the decaying process of those transformed β-phase crystallites was also monitored with unloading the stretching. The relaxation can immediately reverse the phase transition as soon as the stress was reduced. During the relaxation, both α and β phases maintained a high degree of orientation. Quantitatively, the decaying kinetics was examined by the correlation between nominalized fraction of β phase with the stretching stress. It seems that the relaxation-reversed phase transition of PBS follows a similar correlation with the strength of unloading stretching, which was not distinctly

https://doi.org/10.1007/s10118-025-3345-3

influenced by the amount of β phase generated to be relaxed. Notably, β phase completely transformed back to α phase before the stress was fully unloaded.

Conflict of Interests

The authors declare no interest conflict.

Electronic Supplementary Information

Electronic supplementary information (ESI) is available free of charge in the online version of this article at http://doi.org/10.1007/s10118-025-3345-3.

Data Availability Statement

The related data of this paper is data that should not be shared, and can be obtained from the author for reasonable reasons. The author's contact information: zhe.ma@tju.edu.cn.

ACKNOWLEDGMENTS

This work was financially supported by the National Natural Science Foundation of China (No. 52273025).

REFERENCES

1 Xu, S. S.; Zhou, J.; Pan, P. J. Strain-induced multiscale structural evolutions of crystallized polymers: from fundamental studies to recent progresses. *Prog. Polym. Sci*. **2023,** *140*, 101676.
2 Zheng, L. R.; Liu, L.; Shao, C. G.; Wang, W.; Wang, B.; Pan, L.; Li, Y. S.; Ma, Z. Phase transition from tetragonal form II to hexagonal form I of butene-1/4-methyl-1-pentene random copolymers: molecular factor versus stretching stimuli. *Macromolecules* **2019**, *52*, 1188–1199.
3 Wang, W.; Shao, C. G.; Zheng, L. R.; Wang, B.; Pan, L.; Ma, G. Q.; Li, Y. S.; Wang, Y. M.; Liu, C. T.; Ma, Z. Stretching-induced phase transition of the butene-1/ethylene random copolymer: orientation and kinetics. *J. Polym. Sci., Part B: Polym. Phys.* **2018**, *57*, 116–126.
4 Miyasaka, K.; Makishima, K. Transition of nylon 6 γ-phase crystals by stretching in the chain direction. *J. Polym. Sci., Part A: Polym. Chem.* **1967**, *5*, 3017–3027.
5 Schultz, J. W. a. J. M. *In-situ* simultaneous synchrotron small- and wide-angle X-ray scattering measurement of poly(vinylidene fluoride) fibers under deformation. *Macromolecules* **2000**, *33*, 1765–1777.
6 Guo, H.; Zhang, Z. C.; Zhu, Y. Study on the effect of stretching behavior on the properties of PVDF films and mechanism. *Polymer* **2024,** *297*.
7 Zhang, C. B.; Wang, L.; Yang, B.; Zhao, H.; Liu, G. M.; Wang, D. J. Stress-induced solid-solid crystal transition in trans-1,4-polyisoprene. *Chinese J. Polym. Sci.* **2022**, *40*, 256–265.
8 Lu, Y.; Sun, Y. Y.; Chen, R.; Li, X. H.; Men, Y. F. Deformation temperature and lamellar thickness dependency of form I to form III phase transition in syndiotactic polypropylene during tensile stretching. *Chinese J. Polym. Sci.* **2014**, *32*, 1210–1217.
9 Danusso, F.; Gianotti, G. Isotactic polybutene-1: formation and transformation of modification 2. *Die Makromolekulare Chemie* **1965**, *88*, 149–158.
10 Azzurri, F.; Flores, A.; Alfonso, G. C.; Baltá Calleja, F. J. Polymorphism of isotactic poly(1-butene) as revealed by microindentation hardness. 1. kinetics of the transformation. *Macromolecules* **2002**, *35*, 9069–9073.
11 Miyoshi, T.; Mamun, A. Critical roles of molecular dynamics in the superior mechanical properties of isotactic-poly(1-butene) elucidated by solid-state NMR. *Polym. J.* **2012**, *44*, 65–71.
12 Li, Y.; Tang, S.; Pan, M. W.; Zhu, L.; Zhong, G. J.; Li, Z. M. Polymorphic extended-chain and folded-chain crystals in poly(vinylidene fluoride) achieved by combination of high pressure and ion–dipole interaction. *Macromolecules* **2015**, *48*, 8565–8573.
13 Du, C. H.; Zhu, B. K.; Xu, Y. Y. Effects of stretching on crystalline phase structure and morphology of hard elastic PVDF fibers. *J. Appl. Polym. Sci.* **2007**, *104*, 2254–2259.
14 Yang, J. J.; Pan, P. J.; Hua, L.; Zhu, B.; Dong, T.; Inoue, Y. Polymorphic crystallization and phase transition of poly(butylene adipate) in its miscible crystalline/crystalline blend with poly(vinylidene fluoride). *Macromolecules* **2010**, *43*, 8610–8618.
15 Martins, P.; Lopes, A. C.; Lanceros-Mendez, S. Electroactive phases of poly(vinylidene fluoride): determination, processing and applications. *Prog. Polym. Sci.* **2014**, *39*, 683–706.
16 Qiu, Z. B.; Lei, T. P.; Li, S. P.; Cai, X. M.; Yang, K. Insights into polymorphic transition of PVDF during nonsolvent-induced phase separation. *Macromolecules* **2024**, *57*, 1159–1168.
17 Nie, Y. J.; Zhao, W. P.; Chen, X.; Zhang, H.; Hu, J.; Wang, S. J.; Yan, S. K. Different crystallization behaviors of poly(vinylidene fluoride) blended with or coated with cetyltrimethylammonium bromide. *Macromolecules* **2023**, *56*, 8214–8221.
18 Tan, Z. Y.; Fu, C.; Gao, Y. X.; Qian, J.; Li, W. Y.; Wu, X. Y.; Chu, H. Y.; Chen, C. H.; Nie, W.; Ran, X. H. Modifications of gamma poly-(vinylidene fluoride) (γ-PVDF) films by high-energy electron beam irradiation. *Radiat. Phys. Chem.* **2018**, *153*, 258–268.
19 Li, Q. Q.; Wang, G. K.; Liang, Z. X.; Hu, Z. J. Highly transparent and adhesive poly(vinylidene difluoride) films for self-powered piezoelectric touch sensors. *Chinese J. Polym. Sci.* **2022**, *40*, 726–737.
20 Ichikawa, Y.; Noguchi, K.; Okuyama, K. W., J Crystal transition mechanisms in poly(ethylene succinate). *Polymer* **2001,** *42*, 3703-3708.
21 Takahashi, Y.; Sumita, I.; Tadokoro, H. Structural studies of polyethers. IX. planar zigzag modification of poly(ethylene oxide). *J. Polym. Sci., Polym. Phys. Ed.* **1973**, *11*, 2113–2122.
22 Liu, G. M.; Zheng, L. C.; Zhang, X. Q.; Li, C. C.; Jiang, S. C.; Wang, D. J. Reversible lamellar thickening induced by crystal transition in poly(butylene succinate). *Macromolecules* **2012**, *45*, 5487–5493.
23 Liu, G. M.; Zheng, L. C.; Zhang, X. Q.; Li, C. C.; Wang, D. J. Critical stress for crystal transition in poly(butylene succinate)-based crystalline–amorphous multiblock copolymers. *Macromolecules* **2014**, *47*, 7533–7539.
24 Tashiro, K.; Nakai, Y.; Kobayashi, M.; Tadokoro, H. Solid-state transition of poly(butylene terephthalate) induced by mechanical deformation. *Macromolecules* **1980**, *13*, 137–145.
25 Yokouchi, M.; Sakakibara, Y.; Chatani, Y.; Tadokoro, H.; Tanaka, T.; Yoda, K. Structures of two crystalline forms of poly(butylene terephthalate) and reversible transition between them by mechanical deformation. *Macromolecules* **1976**, *9*, 266–273.
26 Zhao, J. Y.; Chen, P. Z.; Lin, Y. F.; Chang, J. R.; Lu, A.; Chen, W.; Meng, L. P.; Wang, D. L.; Li, L. B. Stretch-induced crystallization and phase transitions of poly(dimethylsiloxane) at low temperatures: an *in situ* synchrotron radiation wide-angle X-ray scattering study. *Macromolecules* **2018**, *51*, 8424–8434.
27 Liu, G. M.; Zhang, X. Q.; Wang, D. J. Stress induced reversible crystal transition in polymers. *Polym. Int.* **2015**, *64*, 951–956.
28 Tashiro, K.; Cheng, J.; Ike, M. Stress-induced reversible phase

transition of poly(tetramethylene naphthalate). *Macromolecules* **2003**, *36*, 359–367.
29 Auriemma, F.; De Rosa, C. Time-resolved study of the martensitic phase transition in syndiotactic polypropylene. *Macromolecules* **2003**, *36*, 9396–9410.
30 De Rosa, C.; Auriemma, F.; Corradi, M.; Caliano, L.; Talarico, G. Stress-induced phase transitions in syndiotactic propene–butene copolymers. *Macromolecules* **2008**, *41*, 8712–8720.
31 Zhou, J.; Zheng, Y.; Shan, G. R.; Bao, Y. Z.; Wang, W. J.; Pan, P. J. Stretch-induced α-to-β crystal transition and lamellae structural evolution of poly(butylene adipate-ran-terephthalate) aliphatic–aromatic copolyester. *Macromolecules* **2019**, *52*, 1334–1347.
32 Wang, Y. T.; Jiang, Z. Y.; Wu, Z. H.; Men, Y. F. Tensile deformation of polybutene-1 with stable form I at elevated temperature. *Macromolecules* **2013**, *46*, 518–522.
33 Men, Y. F. Critical strains determine the tensile deformation mechanism in semicrystalline polymers. *Macromolecules* **2020**, *53*, 9155–9157.
34 Chen, G. Q.; Patel, M. K. Plastics derived from biological sources: present and future: a technical and environmental review. *Chem. Rev.* **2012**, *112*, 2082–2099.
35 Barletta, M.; Aversa, C.; Ayyoob, M.; Gisario, A.; Hamad, K.; Mehrpouya, M.; Vahabi, H. Poly(butylene succinate) (PBS): materials, processing, and industrial applications. *Prog. Polym. Sci.* **2022**, *132*, 101579.
36 Tserki, V.; Matzinos, P.; Pavlidou, E.; Panayiotou, C. Biodegradable aliphatic polyesters. part II. synthesis and characterization of chain extended poly(butylene succinate-*co*-butylene adipate). *Polym. Degrad. Stabil.* **2006**, *91*, 377–384.
37 Tserki, V.; Matzinos, P.; Pavlidou, E.; Vachliotis, D.; Panayiotou, C. Biodegradable aliphatic polyesters. part I. properties and biodegradation of poly(butylene succinate-co-butylene adipate). *Polym. Degrad. Stabil.* **2006**, *91*, 367–376.
38 Xu, J.; Guo, B. H. Poly(butylene succinate) and its copolymers: research, development and industrialization. *Biotechnol. J.* **2010**, *5*, 1149–1163.
39 Gigli, M.; Fabbri, M.; Lotti, N.; Gamberini, R.; Rimini, B.; Munari, A. Poly(butylene succinate)-based polyesters for biomedical applications: a review. *Eur. Polym. J.* **2016**, *75*, 431–460.
40 Zhu, C. Y.; Zhang, Z. Q.; Liu, Q. P.; Wang, Z. P.; Jin, J. Synthesis and biodegradation of aliphatic polyesters from dicarboxylic acids and diols. *J. Appl. Polym. Sci.* **2003**, *90*, 982–990.
41 Jacquel, N.; Freyermouth, F.; Fenouillot, F.; Rousseau, A.; Pascault, J. P.; Fuertes, P.; Saint-Loup, R. Synthesis and properties of poly(butylene succinate): efficiency of different transesterification catalysts. *J. Polym. Sci., Part A: Polym. Chem.* **2011**, *49*, 5301–5312.
42 Jin, T. X.; Zhou, M.; Hu, S. D.; Chen, F.; Fu, Q.; Fu, Y. Effect of molecular weight on the properties of poly(butylene succinate). *Chinese J. Polym. Sci.* **2014**, *32*, 953–960.
43 Ichikawa, Y.; Kondo, H.; Igarashi, Y.; Noguchi, K.; Okuyama, K.; Washiyama, J. Crystal structures of *α* and *β* forms of poly(tetramethylene succinate). *Polymer* **2000**, *41*, 4719–4727.
44 Ichikawa, Y.; Washiyama, J.; Moteki, Y.; Noguchi, K.; Okuyama, K. Crystal transition mechanisms in poly(tetramethylene succinate). *Polym. J.* **1995**, *27*, 1230–1238.
45 Tatsuoka, S.; Sato, H. Stress-induced crystal transition of poly(butylene succinate) studied by terahertz and low-frequency raman spectroscopy and quantum chemical calculation. *Spectrochim. Acta, Part A* **2018**, *197*, 95–102.
46 Ichikawa, Y.; Suzuki, J.; Washiyama, J.; Moteki, Y.; Noguchi, K.; Okuyama, K. Strain-induced crystal modification in poly(tetramethylene succinate). *Polymer* **1994**, *35*, 3338–3339.
47 Tashiro, K.; Hu, J.; Wang, H.; Hanesaka, M.; Saiani, A. Refinement of the crystal structures of forms I and II of isotactic polybutene-1 and a proposal of phase transition mechanism between them. *Macromolecules* **2016**, *49*, 1392–1404.
48 Shen, J. Z.; Li, W.; Zhao, R. J.; Liu, Y. Z.; Ma, Z. Utilizing 3-methyl-1-butene co-units to tailor phase transition behavior in butene-1 copolymers. *CrystEngComm* **2024**, *26*, 51–60.
49 Men, Y. F.; Rieger, J.; Strobl, G. Role of the entangled amorphous network in tensile deformation of semicrystalline polymers. *Phys. Rev. Lett.* **2003**, *91*, 095502.

https://doi.org/10.1007/s10118-025-3345-3